Simulation of molecular Auger spectra using a two-electron Dyson propagator

Simulation of molecular Auger spectra using a two-electron Dyson propagator

Y. Hori, M. Nishida, F. H. Lim, T. Ida and M. Mizuno

Chemistry Course, Division of Material Chemistry, Graduate School of Natural Science and Technology, Kanazawa University, Kanazawa 920-1192

Abstract

In order to simulate Auger electron spectra (AES), we propose the use of the two-electron Dyson propagator with the shifted denominator approximation (SD2). The double ionization potentials (DIPs) of molecules calculated using the SD2 method have shown good agreement with experimental data. This method can be used to calculate each DIP separately, and reducing the matrix dimensionality into that of only a two-hole configurations. We carried out AES simulations of water (H_2O), ethylene (C_2H_4), and formaldehyde (H_2CO) molecules and compared with the observed spectra. Furthermore Auger line shapes of glycine and hydrated glycine molecules were simulated, it found out that the peaks of nitrogen *K-LL* Auger were broadened due to hydration. From these results, we conclude that the SD2 method is very useful for the calculation of DIPs to investigate the properties of a double ionized molecule.

Introduction

The double ionization potential (DIP) is defined as the energy required for the detachment of two electrons from a neutral molecule, and these have been studied extensively using a variety of both experimental and theoretical techniques [1,2]. In particular, Auger electron spectra (AES) are widely used in materials science to investigate the properties of neutral and doubly-ionized states of a molecule [3-8]. In early AES studies, the electronic energy difference method based on configuration interaction (*Δ*CI) [9-11] was used. More recently, coupled cluster (CC) [11] or complete active space (CAS) [12,13] methods have been used in theoretical investigations. However, using the *Δ*CI, CC, and CAS methods to calculate doubly-ionized states is difficult for most systems of chemical interest because a number of unnecessary excited states must be included in the calculation.

On the other hand, the particle-particle second-order algebraic diagrammatic construction (ADC(2)) [14-19] has been widely used to theoretically study the double ionization process in molecules. The ADC(2) method is based on analysis of the Feynman diagrams, which describe the second-order perturbation expansion of the electron propagator with respect to the Hartree-Fock determination reference. One advantage of the ADC(2) method is that the advanced and retarded Green's functions are treated separately. The explicit configuration space of ADC(2) comprises main space (two-hole configuration; 2*h*) and subspace (three-hole one-particle configuration; 3*hp*), and a

large matrix representing the entire space must be diagonalized. For example, in the case of a formaldehyde molecule, the number of configurations of $2h$ and $3hp$ space are 36 and 10,080 dimensions, respectively, in a DIPs calculation using the Aug-cc-pVDZ basis set.

In our previous work, in contrast to ADC(2), the second-order two-electron Dyson propagator for the $2h$ configuration renormalizing the other spaces was derived from superoperator theory and applied to the shifted denominator approximation (SD2) [20]. Although the two-particle propagator can be used to simulate Auger spectra, as reported by Ortiz [21] and Liegener [22, 23], our new propagator includes higher order electron correlation terms than the other propagators. The DIPs of small molecules calculated by the SD2 method have shown good agreement with experimental data [20]. However the SD2 method includes both the advanced and retarded functions, namely the causal Green's function or the Dyson propagator, each DIP is calculated separately so that the matrix dimensionality is reduced into only $2h$ configurations. Because these features are advantageous for many-core computing, it is important to investigate the accuracy of AES simulations using the SD2 methods. In this study, we focus on AES simulations of water (H_2O), ethylene (C_2H_4), and formaldehyde (H_2CO) molecules and introduce two-hole population analysis into the SD2 method to evaluate the AES peak intensity. From comparing these simulated spectra with the observed ones, we confirm the validity of our method.

Recently, some relaxation process from the core-hole state, such as intermolecular coulombic decay, have been reported [24, 25]. Auger electron spectroscopy is also a sensitive tool for system concerned with proton-transfer [26]. Unger and co-workers revealed that the proton-transfer-mediated processes were an important role of chemical reactivity in solution by high-accuracy Auger electron spectroscopy measurement for hydrated ammonia and glycine molecules [27]. They, however, didn't directly illustrate the relationship between the measurement and the molecular structure through the AES simulation. Especially, it is a basic subject of interest how AES for the glycine molecule changes in solution. Therefore, in order to clarify that our method can be applied for systems of chemical interest, we simulate Auger spectra of the glycine and the hydrated glycine molecules.

Theoretical background

In order to simulate AES using the two-electron propagator, there are two steps: (1) Calculation of the vertical double ionization potentials (DIPs) and (2) peak intensity calculation. In the experimental AES, the DIPs were obtained from the following equation,

$$E_k = E_{\mathrm{CEBE}} - E_{\mathrm{DIP}} \tag{1}$$

where E_k, E_{CEBE}, and E_{DIP} are the peak position in the Auger spectrum, the core electron binding

energy, and the double ionization energy, respectively. In the AES simulations, by assuming a value of the core electron binding energy, the peak position of the AES spectra can be directly compared with the calculated double ionization energy. Several DIP and peak intensity calculation methods that can be used to simulate AES are described below.

(1) **Vertical double ionization potentials (DIPs)**

In this study, we used the SD2 method to calculate DIPs and simulate AES. A more detailed description of the SD2 method is given in Ref. 20, so we introduce the only critical points here.

The zeroth-order propagator restricts operator averages in the ground state to the Hartree-Fock configuration, and therefore corresponds to the double Koopmans energy. Electron correlation and relaxation effects are considered in the first- and second-order energy-independent and dependent self-energy terms. From the correlation and relaxation terms, we obtained the following explicit expression of the self-energy element of the second-order two-electron Dyson propagator (2nd):

$$
\begin{aligned}
[\mathbf{\Sigma}(E)]_{ij,kl} = &-\langle ij||kl\rangle \\
&+\frac{1}{4}\big(1-P_{ij}\big)(1-P_{kl})\sum_{m,ab}\delta_{jl}\big[\langle im||ab\rangle t_{km,ab}+\langle km||ab\rangle t_{im,ab}\big] \\
&+\frac{1}{2}\sum_{ab}\left[\frac{\langle ij||ab\rangle\langle ab||kl\rangle}{E-\epsilon_a-\epsilon_b}\right]+\big(1-P_{ij}\big)(1-P_{kl}) \\
&\times\left[\frac{1}{2}\delta_{jl}\sum_{m,n,a}\frac{\langle ia||mn\rangle\langle mn||ka\rangle}{E-\big(\epsilon_j+\epsilon_m+\epsilon_n-\epsilon_a\big)}-\sum_{m,a}\frac{\langle ia||lm\rangle\langle jm||ka\rangle}{E-\big(\epsilon_j+\epsilon_l+\epsilon_m-\epsilon_a\big)}\right]
\end{aligned}
\tag{2}
$$

where the indices *i, j* and *a, b* represent occupied and unoccupied spin orbitals, respectively. And P_{ij} is a permutation operator and exchanges indices *i* and *j* in the following term. $t_{im,ab}$ and $\langle ij||kl\rangle$ correspond to the MP2 amplitude and anti-symmetrized Coulomb repulsion. A shifted denominator approximation (SD2) of the self-energy term for the $3hp$ configuration was then obtained from substitution of the following terms,

$$
\big[E-\big(\epsilon_i+\epsilon_j+\epsilon_k-\epsilon_a\big)\big]^{-1}\rightarrow\big[E-\big(\epsilon_i+\epsilon_j+\epsilon_k-\epsilon_a\big)-\big(1+P_{ij}+P_{jk}\big)\{\langle ja||ja\rangle-\langle ik||ik\rangle\}\big]^{-1}
$$

The first order diagonal element from the $3hp$ configuration gives a particular ladder diagram up to infinite order for the second order self-energy. In a practical DIP calculation, we can construct the self-energy matrix by calculating all elements of the $2h$ space, obtaining the diagonal self-energy $[\Sigma(E)]_{ij}$ with respect to *E*. Using a pole search method based on the Dyson equation, a vertical DIP (E_{ij}^{DIP}) with two-hole orbitals *i* and *j* is obtained at the point of convergence using the following equation,

$$E_{ij}^{DIP} = \varepsilon_i + \varepsilon_j + [\Sigma(E_{ij}^{DIP})]_{ij} \qquad (3)$$

where $\varepsilon_i + \varepsilon_j$ is the double Koopmans energy. In the pole search, the pole strength is also obtained. The pole strength indicates the contribution of the two-hole state, which is the main configuration, to the DIP.

(2) **Peak intensity: two-hole population analysis**

For the Auger transition intensities, we employed the two-hole population analysis reported by Tarantelli, Sgamellotti, and Cederbaum [19]. This method is a simple implementation of Mulliken population analysis. We restricted the formulation to the 2*h* components of the eigenvectors in the atomic orbital (AO) basis,

$$\left|ij^{(s,t)}\right\rangle = \sum_{p,q} U_{pq,ij}^{(s,t)} \left|pq^{(s,t)}\right\rangle \qquad (4)$$

where the superscripts *s* and *t* denote singlet and triplet spin multiplicity, respectively, and *ij* and *pq* are MO and AO hole indices, respectively. The matrix elements $U^{(s)}$ and $U^{(t)}$ can be worked out in terms of the HF eigenvector matrix of LCAO coefficients **C**,

$$U_{pq,ij}^{(s,t)} = C_{pi}C_{qj} \pm C_{qi}C_{pj}, \qquad (5)$$

where plus and minus signs are corresponding to singlet and triplet states, respectively. The overlap matrices over the AO 2*h* functions are expressed as

$$O_{pq,rs}^{(s,t)} = S_{pr}S_{qs} \pm S_{ps}S_{qr} \qquad (6)$$

where **S** is the basis set overlap matrix. It is straightforward to express the 2*h* part of the propagator's eigenvector $\mathbf{X}_n$ for the *n*-th two-hole state in terms of the AO 2*h* function. We obtain a new vector $\mathbf{Y}_n$ as follows,

$$\mathbf{Y}_n = \mathbf{U}\mathbf{X}_n \qquad (7)$$

Therefore, the contribution of the AO 2*h* function to the total weight of the *n*-th state is

$$Q_{pq,n} = P_n Y_{pq,n} \sum_{rs} Y_{rs,n} O_{pq,rs} \quad (8)$$

where P_n is the pole strength of the *n*-th two-hole state. For intensities of the triplet final states, the values have been multiplied by factor of 1/3. The sum of terms $Q_{pq,n}$, where both p and q refer to basis functions on a given atom A, is the *one-site* localization hole on A for the *n*-th state. Similarly, we obtain the *two-site* character of a state for each pair of atoms A and B. We will discuss the validity of *one-* and *two-site* characters to the Auger transition intensities.

Computational results and discussion

To investigate the validity of our two derived second-order two-electron Dyson propagator (2nd and SD2) methods for Auger spectral simulation, we calculated the DIPs and simulated oxygen *K-LL* Auger spectra for water, ethylene, and formaldehyde molecules. All calculations were performed using the Aug-cc-pVDZ basis with experimental molecular geometries for small molecules. The geometries of the glycine and the hydrated glycine molecules were optimized by MP2 calculation. Core orbitals were dropped from the 2nd and SD2 propagator summations. Simulated Auger spectra were generated by convoluting a simple Gaussian function with a line width of 2.0 eV and the intensity of the two-hole population with each calculated DIP.

・Water (H_2O) molecule

The water molecule contains the simplest and most important example of a doubly- or multi-ionized electronic state. We began by calculating the DIPs and the two-hole population of water for comparison with the data obtained using the ADC(2) method. Table 1 shows calculated DIPs for the lowest 9 doubly-ionized states of the water molecule, as calculated by the second-order two-electron propagators (2nd and SD2), along with experimental values. DIPs results obtained by the ΔCISD and ADC(2) methods are also listed. The DIPs results from the SD2 method were in good agreement with the experimental results and the ADC(2) results. The SD2 DIPs numbered 1 and 2 in the table were close to those calculated using ΔCISD, which is the most accurate method shown in this table.

Figure 1 shows simulated oxygen *K-LL* Auger spectra of water, obtained using the 2nd and SD2 methods, along with an experimental spectrum. In the figure, the measured kinetic energy of the Auger electrons was subtracted from the core electron binding energy of 542 eV for easier comparison of the simulated and experimental data. Auger spectra simulated by the SD2 method with two-hole population analysis were in good agreement with the experimental spectrum. Note that the two experimental peaks around 40-45 eV had intensities different from the equivalent intensities of the simulated peaks. It has been reported that the integral intensities of the two peaks

were equivalent using ADC(2) [16], but the peak at 45 eV involving $^1A_1$ or $^1A_2$ two-hole states was broadened due to a lifetime-vibrational interference effect of the core-hole state [28]. To put the fact another way, we can get an information of lifetime of the core-hole state by comparing observed peak shape with simulated one. Therefore the validity of our proposed method for Auger spectral simulation of a water molecule is confirmed.

・Ethylene (C_2H_4) molecule

The DIPs of an ethylene molecule were computed for 18 singlet and 15 triplet states in the energy range 30–60 eV. Table 2 shows numerical DIPs results for the lowest 10 doubly ionized states obtained with the SD2, ΔCISD, and ADC(2) methods, along with experimental results. For ethylene, our results were also in good agreement with experimental values and with those obtained using the ADC(2) method. To simulate AES of ethylene, the core-hole localization effect should be considered, as the inner molecular orbital of the ethylene molecule undergoes symmetry breaking in the Auger decay process [29]. Tarantelli et al. reported that one-site character with a two-hole population ADC(2) analysis including the hole localization effect reproduced the experimental Auger line shapes [19]. A previous AES simulation with ADC(2) used 666 two-hole states (276 singlets and 390 triplets) [17], in this study we computed only 33 states, as discussed above. It is necessary to verify whether the two-hole population analysis using the SD2 method can be produced AES peaks of C_2H_4 molecule.

In order to compare our results with the experimental Auger peaks, the core electron binding energy of carbon was fixed at 290 eV. Figure 2 shows the experimental carbon Auger spectra of C_2H_4, simulated spectra with peak intensities determined by (a) only one-site character (C^{2+}=C^0 or C^0=C^{2+}) and (b) both one- and two-site character (C^{1+}=C^{1+}), which is a total two-hole population analysis. The observed spectrum of ethylene had 6 peaks and one broad peak, which is labeled with a * symbol in Fig. 2. Because the broad peak was not due to an Auger decay process [5], it is omitted in the remainder of this discussion. The third peak at 40 eV had the highest intensity in the observed spectrum, and the intensities of peaks after the fourth decreased gradually. Compared with the spectra calculated using the total population (b), that computed with only one-site character (a) is in good agreement with experimental one. Therefore, for an AES simulation of a molecule that undergoes symmetry breaking in the Auger decay process, it is clear that the peak intensities calculated using the SD2 method with only one-site character can be applied in spite of computing the small number of states.

・Formaldehyde (H_2CO) molecule

We carried out AES simulations on formaldehyde as a molecule with heteronuclear core. Figure 3 shows the experimental carbon and oxygen *K-LL* Auger spectra of H_2CO. Two quite different spectra

are observed due to the different localization properties of the molecular orbitals. Previously, detailed spectral features could be described using the ADC(2) treatment [18] with a number of computed DIPs and their line-widths including molecular vibration effects. In this study, the DIPs of a formaldehyde molecule were computed for 21 singlet and 15 triplet states in the energy range from 30 to 70 eV. Table 3 shows numerically obtained DIPs of the lowest 10 doubly-ionized states obtained by the SD2, ΔCISD, and ADC(2) methods, along with experimental values and two-hole population analysis of the one-site character of oxygen and carbon atoms. In the case of formaldehyde, the DIPs obtained by our proposed method are in good agreement with experimental values and those obtained by ΔCISD. It seems that the SD2 results were closer to the experimental values, and may therefore be a more accurate calculation method than ADC(2).

Simulated and observed carbon and oxygen *K-LL* Auger spectra are shown in Figure 3. As can be seen in the figure, for both carbon and oxygen *K-LL* Auger spectra simulations, not only the DIPs results but also the peak intensities obtained using the SD2 method agreed well with the experimental values. In the range of 40–50 eV, where the carbon and oxygen spectra appear very different, the carbon spectrum had a broad band whereas the oxygen spectrum consisted of narrower peaks. It is clear that the simulated spectra successfully reproduced these features. Although the simulated peak at 40 eV involving the $^1A_1$ two-hole state was narrower than the experimental peak, ADC(2) produced similar results [18]. Consequently, we conclude that the SD2 method can be applied to the Auger decay processes of a heteronuclear molecule.

- **Glycine and hydrated glycine molecules**

Although Liegener and co-worker have already reported the AES simulation on glycine and glycine ion molecules in solution by the Green's function [22], their method used only the first-order correlation terms and the point charge model for water molecule. In this study, we employ a complexation of a glycine and a water molecules as the hydrated glycine model. The geometry optimized glycine and the hydrated glycine molecules are shown in Figure 4. The glycine molecule showed plane arrangement of C, N and O atoms. On the other hand, the hydrated glycine was distorted from the plane and holding the water molecule in between O and N atoms. The complexation energy of the hydrated glycine corrected basis set superposition error was -48.7 kJ/mol. Because the complexation energy is more than that of the typical hydrogen bond, it is considered that the glycine and the water molecules are strongly holding and the hydrated glycine make a core cluster in solution.

The DIPs for the glycine and the hydrated glycine were computed for 225 (120 singlets and 105 triplets) and 361 (190 singlets and 171 triplets) two-hole states, respectively. Simulated and observed nitrogen *K-LL* Auger spectra are shown in Figure 5, where the core electron binding energy of nitrogen was fixed at 405 eV. As can be seen in the figure, positions of the peak showed no change,

but the peak shapes were broadened due to hydration. It is considered that a lot of water molecule randomly approach to glycine, the peak shape will be broader than the simulated auger spectrum and close to observed one. Of cause, our method can be also simulated Auger spectra for the ion or zwitterion states, because the number of DIPs is same points for the neutral hydrated glycine. Thus, it is concluded the AES simulation by the SD2 method and the two-hole population analysis can be applied for systems of chemical interest.

Conclusion

A second-order two-electron Dyson propagator with a shifted denominator approximation (SD2) was generally derived based on superoperator theory. Auger spectra simulated with the introduction of two-hole population analysis into the SD2 method for the H_2O, C_2H_4, and H_2CO molecules were in good agreement with the observed spectra. Moreover, it was confirmed from the two-hole population analysis on the one-site character by SD2 that the Auger decay process of the C_2H_4 molecule involves localized double-hole states, and that the process is localized in the heteronucleus of the H_2CO molecule. Furthermore Auger line shapes of the glycine and the hydrated glycine molecules were simulated, it found out that the peaks of nitrogen *K-LL* Auger were broadened due to hydration.

The Dyson propagator can be used to calculate each DIP value separately and reduces the matrix dimensionality into that of only 2*h* configurations, while providing results as accurate as those of ADC(2). We conclude that the SD2 method with two-hole population analysis is very useful for DIPs calculations and the simulation of Auger spectra to investigate the properties of doubly-ionized molecules.

Table 1. Numerically obtained DIPs (eV) of the 9 doubly ionized states of water calculated by 2nd and SD2 two-electron propagator, ΔCISD, ADC(2) [16] results, experimental values [4], and results of two-hole population analysis.

		This work (eV)			ADC(2)	Auger	2h pop.
No.	State	2nd	SD2	ΔCISD			analysis
1	$^3B_1$	33.77	39.76	39.62	38.5	39.1	0.233
2	$^1A_1$	34.35	41.34	40.96	39.6	41.3	0.783
3	$^1B_1$	35.92	42.38		41.2		0.679
4	$^3A_2$	39.08	43.82		42.9		0.155
5	$^1A_1$	39.11	45.79		44.3	46.3	0.567
6	$^1A_2$	39.69	45.76		44.8		0.471
7	$^3B_2$	41.17	45.60		44.8		0.139
8	$^1B_2$	41.98	47.98		47.0		0.417
9	$^1A_1$	47.13	53.25		52.1	53.2	0.291

Table 2. Numerically obtained DIPs (eV) of the 10 doubly ionized states of C_2H_4 along with ADC(2) results [17], experimental values [5], and results of two-hole population analysis for the one-site and two-site characters.

		This work (eV)		ADC(2)	Auger	2h pop. analysis	
No.	State	SD2	ΔCISD			one-site	two-site
1	^1A_g	31.23	30.14	29.46	30.1	0.413	0.411
2	^3A_u	31.50	31.45	30.65		0.039	0.039
3	^1A_u	32.11		31.19		0.118	0.118
4	$^3B_{3u}$	33.89		32.78		0.092	0.092
5	^1A_g	34.76		33.93	34.5	0.009	0.073
6	$^1B_{3u}$	34.93		33.81		0.260	0.260
7	$^3B_{1g}$	35.17		33.73		0.066	0.066
8	$^3B_{3g}$	35.71		34.96		0.029	0.024
9	$^1B_{1g}$	36.11		34.87		0.200	0.200
10	$^3B_{3u}$	36.61		35.92		0.000	0.040

Table 3. Numerically obtained DIPs (eV) of the 10 doubly ionized states of H_2CO, along with ADC(2) results [18], experimental values [6], and the results of two-hole population analysis for the one-site character on oxygen and carbon atoms.

		This work (eV)		ADC(2)	Auger	2h pop. analysis	
No.	State	SD2	ΔCISD			Carbon	Oxygen
1	$^1A_1$	32.67	33.14	31.69	33.8	0.011	0.196
2	$^3A_2$	35.26		34.16		0.014	0.116
3	$^3B_2$	36.23		35.48		0.010	0.113
4	$^1A_2$	36.46		35.47	37.0	0.057	0.281
5	$^3A_1$	36.55	36.46	35.83		0.003	0.000
6	$^1B_2$	38.19		37.23	39.3	0.034	0.236
7	$^1A_1$	40.04		39.07	40.4	0.032	0.425
8	$^3B_2$	40.93		40.10		0.009	0.020
9	$^3B_1$	40.96		39.53		0.024	0.128
10	$^1B_2$	41.80		40.63		0.024	0.009

References

[1] L. Streit, F. B. C. MacHado, R. Custodio, Chem. Phys. Lett., 506 (2011) 22.

[2] J. H. D. Eland, Adv. Chem. Phys., 141 (2009) 103.

[3] H. Siegbahn, L. Asplund, P. Kelfve, Chem. Phys. Lett., 35 (1975) 330-335.

[4] W. E. Moddeman, T. A. Carlson, M. O. Krause, B. P. Pullen, W. E. Bull, G. K. Schweitzer, J. Chem. Phys., 55 (1971) 2317.

[5] R. R. Rye, T. E. Madey, J. E. Houston, P. H. Holloway, J. Chem. Phys., 69 (1978) 1504.

[6] N. Correia, A.N. de Brito, M. P. Keane, L. Karlsson, S. Svensson, C-M. Liegener, A. Cesar, H. Ågren, J. Chem. Phys. 95 (1991) 5187.

[7] R. Feifel, Y. Velkov, V. Carravetta, C. Angeli, R. Cimiraglia, P. Sałek, F. Gel'mukhanov, S. L. Sorensen, M. N. Piancaśtelli, A. De Fanis, K. Okada, M. Kitajima, T. Tanaka, H. Tanaka, K. Ueda, J. Chem. Phys., 128 (2008) 064304.

[8] L. Inhester, C. F. Burmeister, G. Groenhof, H. Grubmüller, J. Chem. Phys., 136 (2012) 144304.

[9] V. R. Saunders J. H. van Lenthe, Mol. Phys., 48 (1983) 923.

[10] H-J. Werner P. J. Knowles, J. Chem. Phys., 89 (1988) 5803.

[11] T. J. Van Huis, S. S. Wesolowski, Y. Yamaguchi1, H. F. Schaefer III, J. Chem. Phys., 110 (1999) 11856.

[12] M. Tashiro, M. Ehara, K. Ueda, Chem. Phys. Lett., 496 (2010) 217.

[13] M. Tashiro, K. Ueda, M. Ehara, Chem. Phys. Lett., 521 (2012) 45.

[14] J. Schirmer, Phys. Rev. A, 26 (1982) 2395.

[15] J. Schirmer A. Barth, Z. Phys. A, 317 (1984) 267.

[16] F. Tarantelli, A. Tarantelli, A. Sgamellotti, J. Schirmer, L. S. Cederbaum, J. Chem. Phys., 83 (1985) 4683.

[17] E. Ohrendorf, H. Köppel, L. S. Cederbaum, J. Chem. Phys., 91 (1989) 1734.

[18] D. Minelli, F. Tarantelli, A. Sgamellotti, L. S. Cederbaum, J. Chem. Phys., 99 (1993) 6688.

[19] F. Tarantelli, A. Sgamellotti, L. S. Cederbaum, J. Chem. Phys., 94 (1991) 523.

[20] T. Ida, J. V. Ortiz, J. Chem. Phys., 129 (2008) 084105.

[21] J. V. Ortiz, J. Chem. Phys., 83 (1985) 4604.

[22] C-M. Liegener, A. K. Bakhshi, R. Chen, J. Ladik, J. Chem. Phys., 86 (1987) 6039.

[23] C-M. Liegener, J. Chem. Phys., 104 (1995) 2940.

[24] L. S. Cederbaum, J. Zobeley, F. Tarantelli, Phys, Rev, Lett., 79 (1997) 4778.

[25] U. Hergenhahn, J. Electron Spectrosc. Relat. Phenom., 184 (2011) 78.

[26] N. V. Kryzhevoi, L. S. Cederbaum, J. Phys. Chem. Lett., 3 (2012) 2733.

[27] I. Unger, D. Hollas, R. Seidel, S. Thürmer, E. F. Aziz, P. Slavíček, B. Winter, J. Phys. Chem. B, 119 (2015) 10750.

[28] A. Cesar, H. Ågren, V. Carravetta, Phys. Rev. A, 40 (1989) 187.

[29] M. S. Schöffler, J. Titze, N. Petridis, T. Jahnke, K. Cole, L. Ph. H. Schmidt, A. Czasch, D. Akoury, O. Jagutzki, J. B. Williams, N. A. Cherepkov, S. K. Semenov, C. W. McCurdy, T. N. Rescigno, C. L. Cocke, T. Osipov, S. Lee, M. H. Prior, A. Belkacem, A. L. Landers, H. Schmidt-Böcking, Th. Weber, R. Dörner, Science, 320 (2008) 920-923.

Figure Captions

Figure 1. Simulated and observed oxygen *K-LL* Auger spectra [4] of a water molecule. For the simulated spectra, the DIPs were calculated using the SD2 and 2nd methods.

Figure 2. Simulated and observed carbon *K-LL* Auger electron spectra [5] of C_2H_4. The intensities were determined by the one-site character and the total two-hole population in the simulated spectra.

Figure 3. Simulated and observed carbon and oxygen *K-LL* Auger spectra [6] of H_2CO.

Figure 4. Optimized geometries for (a) glycine and (b) complexation of a glycine and a water molecules as the hydrated glycine model. The values in figure (b) indicate distance of the hydrogen bond.

Figure 5. Simulated and observed nitrogen *K-LL* Auger spectra [27] of the glycine (upper) and the hydrated glycine (lower). Observed blue and red lines are corresponding to the glycine in H_2O and D_2O solvent, respectively, and details in Ref. 27.

Figure 1

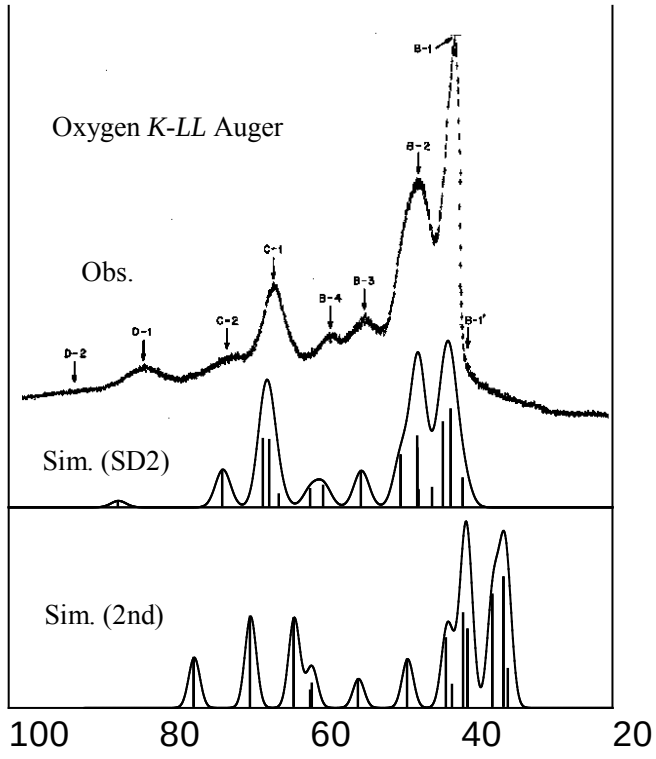
Oxygen *K-LL* Auger
Obs.
Sim. (SD2)
Sim. (2nd)
B-1
B-2
B-3
B-4
B-1'
C-1
C-2
D-1
D-2
100
80
60
40
20
DIPs (eV)

Figure 2

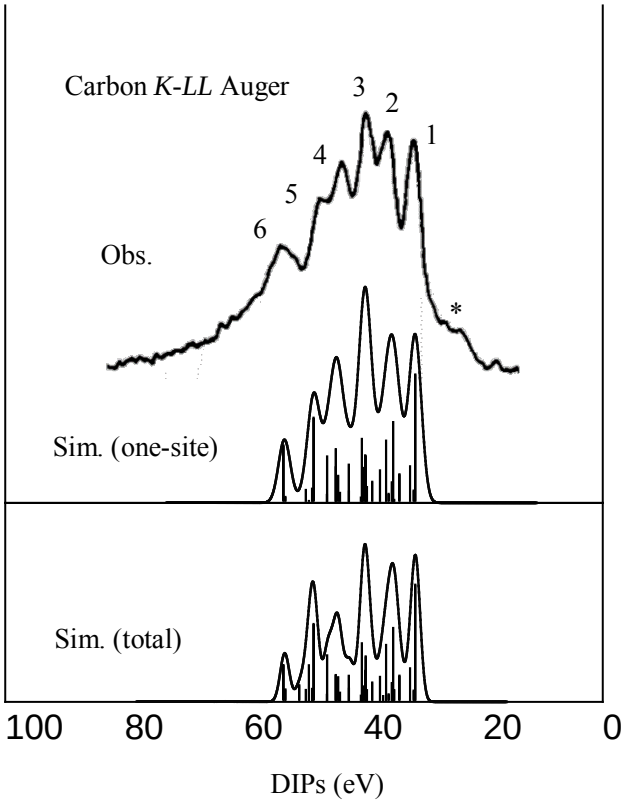
Carbon K-LL Auger
3
2
1
4
5
6
Obs.
*
Sim. (one-site)
Sim. (total)
100
80
60
40
20
0
DIPs (eV)

Figure 3

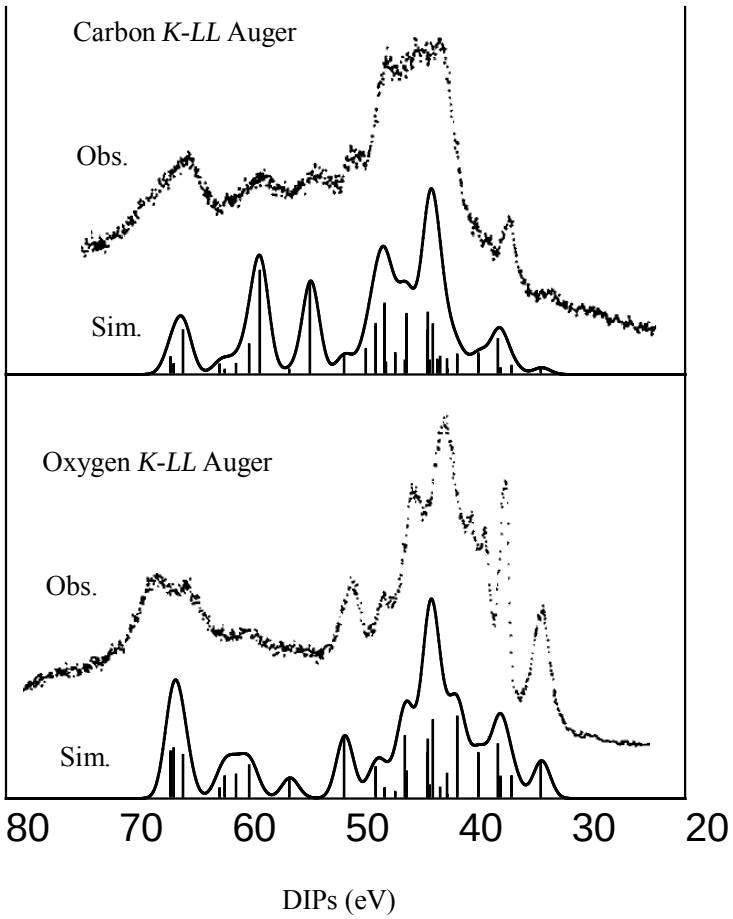
Carbon *K-LL* Auger
Obs.
Sim.
Oxygen *K-LL* Auger
Obs.
Sim.
80
70
60
50
40
30
20
DIPs (eV)

Figure 4

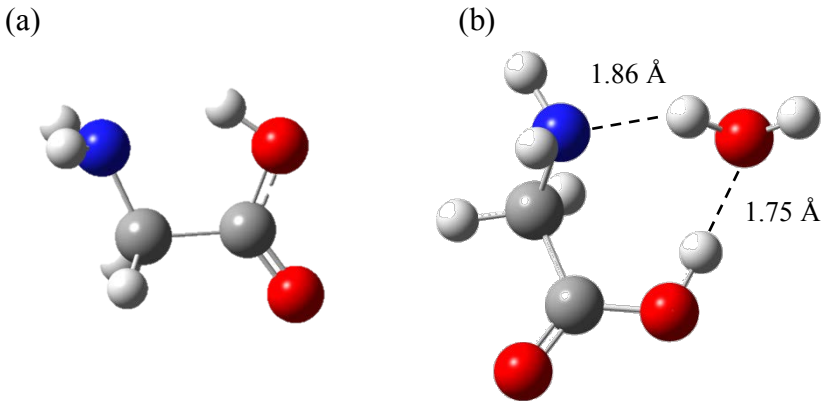

Figure 5

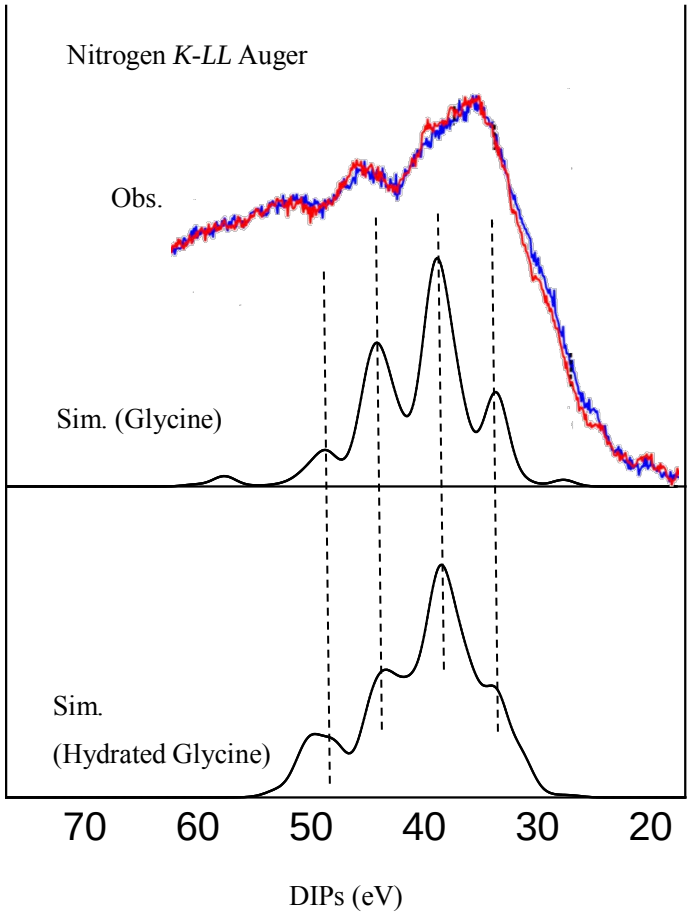
Nitrogen *K-LL* Auger
Obs.
Sim. (Glycine)
Sim.
(Hydrated Glycine)
70
60
50
40
30
20
DIPs (eV)